

Autonomous Distributed Control of Traffic Signals with Cycle Length Control[†]

Masao SUGI*, Hideo YUASA**,
Jun OTA*** and Tamio ARAI***

A new method is proposed for controlling a large number of traffic signals, which are represented by nonlinear oscillators, each governed by a reaction-diffusion equation at a node of a graph. The behavior of each signal is determined only by the states of its neighbors, with the system as a whole being also organized globally. In this report, cycle lengths of the signals are controlled according to the traffic condition. Along with the control of offsets and splits, which are also explained here, the system can achieve high performance in dynamic traffic conditions. The simulation results are exemplified to show the validity of the method.

Key Words: traffic signal, wide area control, cycle length, nonlinear coupled oscillator system, reaction-diffusion equation on a graph

1. Introduction

Growing number of automobiles deteriorates traffic conditions and brings forth increased congestion and more frequent accidents. The control of traffic signals [2] has been researched as one of the countermeasures to improve such situations.

In the traffic signal control, three parameters, the cycle length (i.e. period of the signal), the split (duty ratio of the green light duration for each direction) and the offset (difference between the onset times of green lights of neighboring signals), are determined according to the traffic conditions. There are two schemes in the traffic control; the isolated control and the coordinated control. The former deals with only one signal, and controls cycle length and split of the signal. Its neighbors are not taken into account. The latter aims at coordinating multiple signals neighboring one another on the same road, and controls the offsets among them, along with the cycle lengths and the splits. This can be expected to achieve

more effective performance than the isolated control. Extension of the coordinated control from one single road to network is often called the wide area control, which can achieve higher performance than the usual coordinated control on a single road.

In the conventional traffic signal control method, a solution of an optimization problem obtained through off-line planning gives the behavior of the signals, which are controlled by a central computer. This method, however, cannot follow dynamic changes of the traffic condition. Recent studies [1, 6] propose real-time control method, replacing the off-line planning in the above method with the on-line one. Although this method can cope with the dynamic changes of the traffic condition, application of it to a large number of traffic signals is limited, because the computation order for calculating the optimal set of parameters over all of the signals will exceed the power of the central computer.

On the other hand, wide area control of traffic signals by the distributed manner [4, 5, 7, 8, 10, 3] has been studied in this decade. This method is more suitable for large size environment with dynamic changes of traffic conditions.

There are several studies that deal with control of a large number of traffic signals by the decentralized method. Mikami et al. [7] and Misawa et al. [8] apply the multi-agent reinforcement learning to control of the split of each signal. The offsets and cycle lengths are not controlled. Lee et al. [10] introduces a distributed fuzzy controller to regulate three parameters. This method, however, assuming no communication between the neighboring signals, cannot control the offsets between the sig-

[†] This research is presented at the 15th SICE Symposium on Decentralized Autonomous Systems, Sendai, Japan, Jan. 2003.

* School of Information Science and Technology, The University of Tokyo, Hongo, Bunkyo-ku, Tokyo

** School of Engineering, The University of Tokyo, Hongo, Bunkyo-ku, Tokyo / Bio-mimetic Control Research Center, RIKEN, Anagahora, Simo-shidami, Moriyama-ku, Nagoya

*** School of Engineering, The University of Tokyo, Hongo, Bunkyo-ku, Tokyo

(Received October 18, 2002)

(Revised April 14, 2003)

nals. In Ref. [4] by Sekiyama et al., a traffic network is modeled using nonlinear coupled oscillators with individual frequency of oscillations. The offset control method using the entrainment phenomena and the split control method are proposed. The cycle length and the offset of each signal, however, cannot be controlled independently of each other, since the both are treated inseparable in that model. Nishikawa et al. [5] adopts oscillators with a fixed common frequency, which is the common characteristic to our oscillator model [3]. Although the control of offsets is dealt with in a generalized manner in [5], the splits and cycle lengths of the signals are not handled in this paper. Thus, wide area control of traffic signals by the decentralized method remains to be developed.

In a previous paper [3], we have also proposed a decentralized signal control method based on the oscillators governed by a reaction-diffusion equation on a graph [9]. Each signal with a fixed common cycle length determines the split and offset from its local traffic conditions. Recently we have extended the previous method by introducing the control of cycle length. The results are shown in this paper.

In section 2, the presumptions of this research are introduced. The method for controlling the splits of signals and the offsets between neighboring signals is explained. In section 3, the concept of closed-loop constraints of the offsets is argued. The cycle length control method is proposed, aiming for relaxation of the closed-loop constraints of the offsets. Some simulation results are discussed in section 4. We conclude this paper in section 4. We conclude this paper in section 5.

2. Autonomous decentralized control of traffic signals

In this section, presumptions of this research are shown at first. This section also describes the control method of the splits of signals and the offsets between neighboring signals, which are basically the same in the previous paper [3]. Therefore the explanation here is kept at a minimum, making the difference to Ref. [3] clear.

2.1 Presumptions

In the present method, automobiles are assumed to go straight in an intersection and turn neither right nor left. The roads are limited to be bidirectional two-lane road, and all the intersections are crossroads (see Fig. 1-(a)). The cycle system of the signals is a 2-phase cycle: “Phase1” for the traffic flows from east and west and “Phase2” from north and south, as shown in Fig. 1-(b).

Each signal can measure the traffic volume (i.e., num-

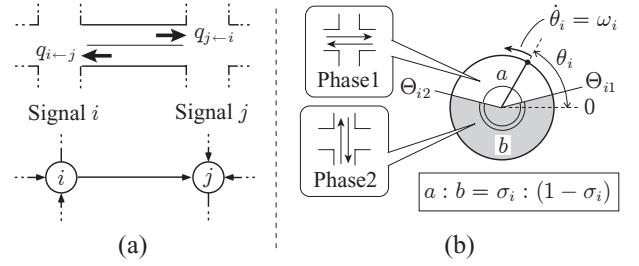


Fig. 1 (a) Traffic volume and oriented graph model. (b) Traffic signal model.

ber of automobiles) from each of four directions, which is shown in Fig. 1-(a). The traffic volume is normalized into $q \in [0, 1]$ using the maximal volume. As shown in Fig. 1-(a), two neighboring signals i and j share the information on $q_{i \leftarrow j}$ (flow volume from j to i) and $q_{j \leftarrow i}$ (volume from i to j).

2.2 Traffic signal model

In this paper, the state of a signal i is described by two variables: the phase angle $\theta_i \in [0, 2\pi)$ and the split $\sigma_i \in [0, 1]$, which is shown in Fig. 1-(b). Here the split σ_i is defined as,

$$\sigma_i = \frac{\tau_{\text{phase1}}}{\tau_{\text{phase1}} + \tau_{\text{phase2}}}, \quad (1)$$

where τ_{phase1} and τ_{phase2} are the time duration of “Phase1” and “Phase2”, respectively.

The actual phase of a signal i is determined using the phase angle θ_i and the split σ_i . Let us first define the phase switch points Θ_{i1} and Θ_{i2} , shown in Fig. 1-(b), i.e.,

$$\Theta_{i1} = \left(\frac{1}{2} - \sigma_i\right)\pi, \quad \Theta_{i2} = \left(\frac{1}{2} + \sigma_i\right)\pi. \quad (\text{mod } 2\pi) \quad (2)$$

Then the phases are determined by Θ_{i1} and Θ_{i2} ;

$$\text{Phase1: } \sin \theta_i \geq \sin \Theta_{i1}, \quad \theta_i \neq \Theta_{i2}, \quad (3)$$

$$\text{Phase2: } \sin \theta_i \leq \sin \Theta_{i2}, \quad \theta_i \neq \Theta_{i1}.$$

The connection (i.e. neighboring relation) of traffic signals is modeled as an oriented graph $G = (V, E)$. It is noted that the direction of each link does not represent that of traffic flow on the link. All the traffic flow is bidirectional. We define a function defined on a link (i, j) as,

$$\text{sign}(i, j) = \begin{cases} 1, & \text{if } i \text{ is the end point of } (i, j), \\ -1, & \text{if } i \text{ is the origin of } (i, j). \end{cases} \quad (4)$$

Using this function, the differences, $\rho_{(i,j)}$ and $\phi_{(i,j)}$, of splits and phase angles, respectively, between neighboring signals i and j , are defined as,

$$\rho_{(i,j)} = \text{sign}(i, j)(\sigma_i - \sigma_j), \quad (5)$$

$$\phi_{(i,j)} = \text{sign}(i, j) \left[\{ \theta_i - \xi(i, (i, j)) \} - \{ \theta_j - \xi(j, (j, i)) \} \right], \quad (6)$$

where $\xi(i, (i, j))$ is a function defined on a node i and a

link (i, j) ,

$$\xi(i, (i, j)) = \begin{cases} \Theta_{i1}, & \text{if a road } (i, j) \text{ goes} \\ & \text{east and west,} \\ \Theta_{i2}, & \text{if a road } (i, j) \text{ goes} \\ & \text{north and south.} \end{cases} \quad (7)$$

It is noted that the difference of phase angles ϕ is defined using angles measured from the phase switch point (Θ_{i1} or Θ_{i2}) as the reference point, instead of the origin, all of which are shown in Fig. 1-(b).

From now on, the variables with subscript (i, j) (e.g. $\rho_{(i,j)}$, $\phi_{(i,j)}$ and so on) is regarded to be defined on the link (i, j) . Because we model road network as a simple graph, not a multiple graph, (i, j) and (j, i) means the same link. Therefore the reciprocal relations, $\rho_{(i,j)} = \rho_{(j,i)}$ and $\phi_{(i,j)} = \phi_{(j,i)}$, hold. On the other hand, the reciprocal relation does not hold on the variables with subscript $i \leftarrow j$, which represents the value related to the traffic flow from the signal i to j .

2.3 Split control

We introduce the following dynamics of σ_i governed by the gradient system,

$$\frac{d\sigma_i}{dt} = -\frac{\partial}{\partial \sigma_i}(W_0 + W_1), \quad (8)$$

where the potentials W_0 and W_1 are given as,

$$W_0 = \sum_{i \in V} \alpha \left(\sigma_i - \frac{q_{i \leftarrow w(i)} + q_{i \leftarrow e(i)}}{\sum_{j \sim i} q_{i \leftarrow j}} \right)^2, \quad (9)$$

$$W_1 = \sum_{i \in V} \sum_{j \sim i} \beta (q_{i \leftarrow j} + q_{j \leftarrow i}) \cdot (\rho_{(i,j)})^2. \quad (10)$$

In the above, $w(i)$ and $e(i)$ denote the west and east neighboring signals of i , respectively. $i \sim j$ denotes that the signal j is a neighbor of i . α and β are parameters to control the speed of convergence.

2.4 Offset control

In order to control the offsets (second as a unit) of signals, we control the difference of phase angles (radian as a unit). We introduce the following gradient system to the oscillators' phase angles,

$$\frac{d\theta_i}{dt} = \omega_i - \frac{\partial V}{\partial \theta_i}, \quad (11)$$

$$V = \sum_{i \in V} \sum_{j \sim i} \left\{ -\gamma_{(i,j)} |q_{i \leftarrow j} - q_{j \leftarrow i}| \times \cos(\phi_{(i,j)} - D_{(i,j)}) \right\}, \quad (12)$$

where ω_i is the oscillation frequency that gives the cycle length of the signal i . $\gamma_{(i,j)}$ is a parameter to control the speed of convergence.

$D_{(i,j)}$ in (12) is the desired value of the difference of phase angles. When $\omega_i = \omega_j$ holds, the difference of the phase angles $\phi_{(i,j)}$ will converge into $D_{(i,j)}$. Here $D_{(i,j)}$ is defined. First we consider only one direction from the two

counter-directional traffic flows on the road (i, j) , and give the desired phase angle difference for this direction. Let us denote the desired difference corresponding the flow $i \leftarrow j$ as $D_{i \leftarrow j}$, and the one corresponding the flow $j \leftarrow i$ as $D_{j \leftarrow i}$. Using v_{\max} , the maximal speed of the automobiles, and $L_{(i,j)} = L_{(j,i)}$, the distance between signals i and j , $D_{i \leftarrow j}$ and $D_{j \leftarrow i}$ are given as,

$$D_{i \leftarrow j} = -\text{sign}(i, j) \frac{\bar{\omega}_{(i,j)} L_{(i,j)}}{v_{\max}}, \quad (13)$$

$$D_{j \leftarrow i} = -\text{sign}(j, i) \frac{\bar{\omega}_{(j,i)} L_{(j,i)}}{v_{\max}}. \quad (14)$$

where $\bar{\omega}_{(i,j)}$ is the mean value of the oscillation frequencies of i and j ,

$$\bar{\omega}_{(i,j)} = \frac{\omega_i + \omega_j}{2}. \quad (15)$$

When $\omega_i = \omega_j = \bar{\omega}_{(i,j)}$ holds, the actual offset between signals i and j is given as $\phi_{(i,j)}/\bar{\omega}_{(i,j)}$. Therefore (13) and (14) show that the desired offset is given as $L_{(i,j)}/v_{\max}$, the necessary time to pass through the road (i, j) .

Next, using the desired phase angle differences of two counter-directional traffic flows (i.e. $D_{i \leftarrow j}$ and $D_{j \leftarrow i}$), we define the desired phase angle difference between i and j with both of two traffic flows taken into account as,

$$D_{(i,j)} = \begin{cases} D_{i \leftarrow j}, & (q_{i \leftarrow j} \geq q_{j \leftarrow i}) \\ D_{j \leftarrow i}, & (q_{i \leftarrow j} < q_{j \leftarrow i}) \end{cases} \quad (16)$$

Equation (16) means that $D_{(i,j)}$ chooses the desired phase angle difference suitable for the direction with larger traffic volume, comparing the two counter-directional traffic flows on the road (i, j) .

2.5 Modification of control method in [3]

Here we state the difference between the previous paper [3] and the present paper.

Instead of the ω_i in (11), we have supposed that the signals have a fixed common frequency of oscillation ω in the previous paper [3]. Furthermore, V in (12) have been given in [3] as,

$$V = \sum_{i \in V} \sum_{j \sim i} \left\{ -\gamma (q_{i \leftarrow j} + q_{j \leftarrow i}) \cos(\phi_{(i,j)} - D_{(i,j)}) \right\}. \quad (17)$$

$D_{(i,j)}$ in (16) have been given in [3] as the weighted interior division of $D_{i \leftarrow j}$ and $D_{j \leftarrow i}$, i.e.,

$$D_{(i,j)} = \begin{cases} 0, & (q_{i \leftarrow j} = q_{j \leftarrow i} = 0) \\ \frac{q_{i \leftarrow j} D_{i \leftarrow j} + q_{j \leftarrow i} D_{j \leftarrow i}}{q_{i \leftarrow j} + q_{j \leftarrow i}}, & (|D_{i \leftarrow j} - D_{j \leftarrow i}| \leq \pi) \\ \pi + \frac{1}{q_{i \leftarrow j} + q_{j \leftarrow i}} \times \left[q_{i \leftarrow j} \{ D_{i \leftarrow j} + \text{sign}(i, j) \pi \} + q_{j \leftarrow i} \{ D_{j \leftarrow i} + \text{sign}(j, i) \pi \} \right], & (|D_{i \leftarrow j} - D_{j \leftarrow i}| > \pi) \end{cases} \quad (18)$$

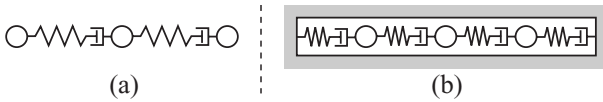


Fig. 2 Analogy to mass-spring-dashpot mechanical systems.

The three branches of the right term in (18) are due to the property of the toroidal $\text{mod } 2\pi$ space, where the interior division between two points appears on the shorter side of the two arc between the two points.

These modifications are necessary for the control of cycle length. The reason of this will be described in the next section.

3. Closed-loop constraints on offsets and cycle length control

3.1 Outline of the cycle length control

In any given loop (or circuit) on a graph, the sum of the offsets between neighboring signals is equal to the integer multiple of the cycle length. This is known as *closed-loop constraint on offsets* [2] in traffic engineering. In general, for n links on a loop, the number of the links with linear independent offsets is only $n - 1$. If we determine the respective offsets of the $n - 1$ links, the offset of the last one link is automatically determined. This means that we cannot design the desired offsets of all of the links arbitrarily.

In the oscillator model, the closed-loop constraint on offsets means that the sum of the difference of the phase angles is equal to $2n\pi$ for $n \in \mathbb{Z}$. Although the phase angle difference $\phi_{(i,j)}$ in (6) (or phase angles θ_i) always satisfies the closed-loop constraint, the desired difference $D_{(i,j)}$ in (16) does not always. When the sum of $D_{(i,j)}$ on a loop does not satisfy the closed-loop constraint, the difference of phase angles $\phi_{(i,j)}$ cannot converge to its desired value $D_{(i,j)}$. The offsets cannot be controlled appropriately in this case.

For this problem, we control the cycle lengths of the signals on a loop into the appropriate value so that the sum of the desired offsets on the loop can satisfy the closed-loop constraint. In fact, if the cycle length of a loop is equal to the quotient of the sum of the desired offsets on the loop divided by any positive integer, the closed-loop constraint is satisfied. Because the desired offsets will change according to the traffic conditions, the cycle length will be changed. By controlling the cycle length, all of the offset values on a signal network can be converged into their respective desired values, and the traffic efficiency will be improved than in the case with fixed cycle length.

Analogy to mass-spring-dashpot mechanical systems⁽¹⁾ in Fig. 2 makes the concept of cycle length control clear. The distance between the material points in the mass-spring-dashpot systems corresponds to the offset of the signals. The natural length of the spring corresponds to the desired offset. In a mechanical system shown in Fig. 2-(a), each distance between two neighboring material points will converge into the natural length of the spring as $t \rightarrow \infty$. This corresponds to the case in which the graph has no loop and there are no closed-loop constraints on offsets. In a system confined to a rigid box, shown in Fig. 2-(b), each distance between neighboring material points will never converge to the spring's natural length as $t \rightarrow \infty$, except that the total of the natural length of the springs is equal to the length of the box. This corresponds to the case we must take the closed-loop constraint on a loop into consider. In this context, our cycle length control method means for changing the length of the box to the sum of the natural lengths of springs.

Although the closed-loop constraint exists on each loop on the graph, the possible loops on a graph are generally too many to take all of them into account. Here, we consider only the *bounded faces*, shown in Fig. 3-(a).

In elaborating the model, we must settle the conflict between the common cycle length and the local optimal cycle length of each loop dependent on the shape and size of the loop. For controlling the offsets between the neighboring signals, $\omega_i \simeq \omega_j$ for all signals is required. We choose a common cycle length that is “reasonable” for most of the loops on the graph.

In this paper, we introduce a new kind of agent “*loop manager*,” which corresponds to each of the bounded faces of the graph, as shown in Fig. 3. Each loop manager l^* changes Ω_{l^*} , the frequency of oscillation of the loop, so that the sum of $D_{(i,j)}$ on the loop l^* may satisfy the closed-loop constraint. At the same time, each loop manager l^* smoothes off the value of Ω_{l^*} , changing it toward the average value of the neighboring loops (i.e. loops which share at least one link of G with the loop l^*). As a result, homogenized value of the frequency of oscillation is obtained. Each signal uses the homogenized value for its frequency of oscillation.

Let us denote the dual graph of G as $G^* = (V^*, E^*)$. The network of the loop managers \tilde{G}^* is defined as,

$$\tilde{G}^* = (\tilde{V}^*, \tilde{E}^*) := \left(V^* \setminus \{v_{\text{inf}}^*\}, E^* \setminus E^*(v_{\text{inf}}^*) \right) \quad (19)$$

(1) Strictly speaking, the dynamics of the gradient system is different from that of the mass-spring-dashpot mechanical system. There is no overshoot in the gradient system.

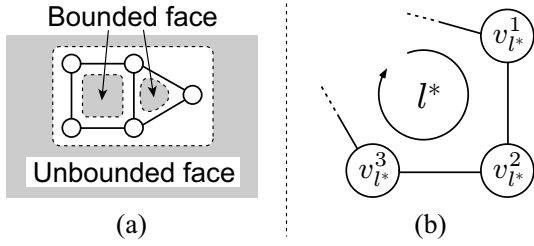


Fig. 3 (a) Bounded and unbounded faces of a graph. (b) Numbered nodes $v_{l^*}^i$ on the loop l^* .

where $v_{\text{inf}}^* \in V^*$ is a node on G^* corresponding to the *unbounded face* on G , and $E^*(v_{\text{inf}}^*) \subset E^*$ is a set of links that are connected to the node v_{inf}^* . We use a subscript “*” for representing a loop on G hereafter. It is noted that a loop on G corresponds to a node on \tilde{G}^* . In this paper, we design the dynamics of loop managers using the reaction-diffusion equation on a graph \tilde{G}^* .

Hereafter we call the graph \tilde{G}^* as “dual graph of G ,” instead of the graph G^* . The term “loop” is regarded as equivalent to a bounded face without notice.

While the reaction-diffusion equation on the dual graph \tilde{G}^* gives the dynamics of the oscillation frequency at nodes on \tilde{G}^* (i.e. oscillation frequency at every loops on G), what is necessary for us is the dynamics of oscillation frequency at nodes on G . The transformation from the oscillation frequency on \tilde{G}^* to the one on G is therefore necessary. In this paper, we introduce the reaction-diffusion equation of oscillation frequency at nodes on G , in which the desired oscillation frequency of each node is determined by the frequencies of the loops nearby.

Figure 4 shows the schematic view of the present method for controlling the cycle lengths of the signals. The left figure of Fig. 4 represents the relations between the signals and the loop managers. As mentioned previously, the network of the loop managers composes a dual graph of the network of the signals. The right figure shows the communication between the signal i_1 and the loop manager l_1^* . The signal i_1 informs the respective values of its phase angle θ_{i_1} , split σ_{i_1} , the traffic volumes $q_{i_1 \leftarrow i_2}$ and $q_{i_1 \leftarrow i_3}$ to the loop manager l_1^* . The loop manager l_1^* , considering these values, determines $\Omega_{l_1^*}$, the oscillation frequency of the loop, and informs it to the signal i_1 . The signal i_1 then changes its own oscillation frequency ω_{i_1} , referring to the value of $\Omega_{l_1^*}$.

It is noted that the communication between the signals and the loop agents is not limited to one to one. The loop manager communicates with all of the signals on the loop (e.g., i_2 and i_3 in Fig. 4). Similarly, each signal communi-

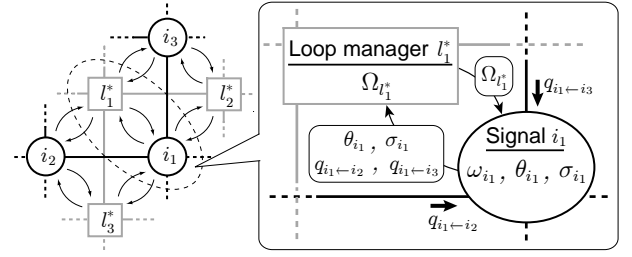


Fig. 4 Schematic view of the present method for the control of the cycle length. Left: Relations between the signals and the loop managers. Right: Communication between signal i_1 and loop manager l_1^* .

cates with all of the loop managers concerned with itself (e.g., l_2^* and l_3^* in Fig. 4).

3.2 Solution of cycle length satisfying closed-loop constraints

Let us obtain the local optimal solution of the loop’s frequency of oscillation for the sum of D satisfying the closed-loop constraint.

From here, we refer to the clockwise orientation circulating the loop l^* as *positive orientation* of l^* . The set of the nodes (i.e. signals) on the loop l^* is denoted by $V(l^*) \subset V$. The elements $v_{l^*}^i \in V(l^*)$ ($i = 1, 2, \dots, |V(l^*)|$) are numbered in accordance with the positive orientation of l^* , as shown in Fig. 3-(b).

Let us denote the frequency of the loop l^* by Ω_{l^*} , which is assumed to be common to all signals on the loop l^* , i.e.,

$$\omega_{v_{l^*}^i} = \Omega_{l^*}, \quad i = 1, 2, \dots, |V(l^*)|. \quad (20)$$

For the neighboring nodes $v_{l^*}^{i-1}, v_{l^*}^i \in V(l^*)$, the following relation holds,

$$\bar{\omega}_{(v_{l^*}^{i-1}, v_{l^*}^i)} = \bar{\omega}_{(v_{l^*}^i, v_{l^*}^{i-1})} = \Omega_{l^*}, \quad i = 1, 2, \dots, |V(l^*)|, \quad (21)$$

and the closed-loop constraint is represented by,

$$\sum_{i=1}^{|V(l^*)|} (\theta_{v_{l^*}^{i-1}} - \theta_{v_{l^*}^i}) = 2n\pi, \quad n \in \mathbb{Z}, \quad (22)$$

where $v_{l^*}^0 \equiv v_{l^*}^{|V(l^*)|}$.

Our aim is to obtain the condition of $D_{(k,h)}$ ($k, h \in V(l^*)$) for satisfying the closed-loop constraint. Let us first introduce $\phi_{(k,h)}$ to rewrite (22). Substituting (7) and (2) for the term of ξ in (6), the relation between θ and ϕ is derived as,

$$\phi_{(i,j)} = \text{sign}(i,j) \{ (\theta_i - \theta_j) - \Delta(i,j, (i,j)) \} \quad (23)$$

where $\Delta(i,j, (i,j))$, a function defined on two nodes $i, j \in V$ and a link (i.e. road) $(i,j) \in E$, is a correction

term,

$$\Delta(i, j, (i, j)) = \begin{cases} -(\sigma_i - \sigma_j)\pi, & \text{if the link } (i, j) \text{ extends east and west,} \\ +(\sigma_i - \sigma_j)\pi, & \text{if the link } (i, j) \text{ extends north and south.} \end{cases} \quad (24)$$

The transformation of the phase angle differences from $\theta_i - \theta_j$ (the difference in the original frame of reference) to $\phi_{(i,j)}$ (the difference with the phase change points as the reference points) brings the correction term $\Delta(i, j, (i, j))$, which is shown in Fig. 5. While (22) is represented by $\theta_i - \theta_j$, the actual parameter of offset control in (12) is $\phi_{(i,j)}$. This is the reason why the correction term is necessary. The value of the correction term $\Delta(i, j, (i, j))$ depends on σ_i and σ_j , the splits of i and j . It is noted that $\Delta(i, j, (i, j)) = 0$ and $\phi_{(i,j)} = \theta_i - \theta_j$ hold when $\sigma_i = \sigma_j$.

We obtain the following formula from (23) and (22),

$$\sum_{i=1}^{|V(l^*)|} \left\{ \text{sign}(v_{l^*}^{i-1}, v_{l^*}^i) \cdot \phi_{(v_{l^*}^{i-1}, v_{l^*}^i)} + \Delta(v_{l^*}^{i-1}, v_{l^*}^i, (v_{l^*}^{i-1}, v_{l^*}^i)) \right\} = 2n\pi, \quad n \in \mathbb{Z}. \quad (25)$$

In deriving the above equation, we used $\text{sign}(i, j)^2 = 1$ for $\forall (i, j) \in E$. Replacing $\phi_{(v_{l^*}^{i-1}, v_{l^*}^i)}$ in (25) with $D_{(v_{l^*}^{i-1}, v_{l^*}^i)}$, we obtain the condition that the desired difference of phase angles D should satisfy,

$$\sum_{i=1}^{|V(l^*)|} \left\{ \text{sign}(v_{l^*}^{i-1}, v_{l^*}^i) \cdot D_{(v_{l^*}^{i-1}, v_{l^*}^i)} + \Delta(v_{l^*}^{i-1}, v_{l^*}^i, (v_{l^*}^{i-1}, v_{l^*}^i)) \right\} = 2n\pi. \quad (26)$$

It is noted that (26) does not always hold, while (25) always does. When (26) holds, the difference of phase angle ϕ converges to its desired value D .

From (16), (13), and (14), we get

$$\text{sign}(i, j)D_{(i,j)} = \begin{cases} -\frac{\bar{\omega}_{(i,j)} L_{(i,j)}}{v_{\max}}, & (q_{i \leftarrow j} \geq q_{j \leftarrow i}) \\ +\frac{\bar{\omega}_{(j,i)} L_{(j,i)}}{v_{\max}}, & (q_{i \leftarrow j} < q_{j \leftarrow i}) \end{cases} \quad (27)$$

Substituting (21) for (27), the following equation is ob-

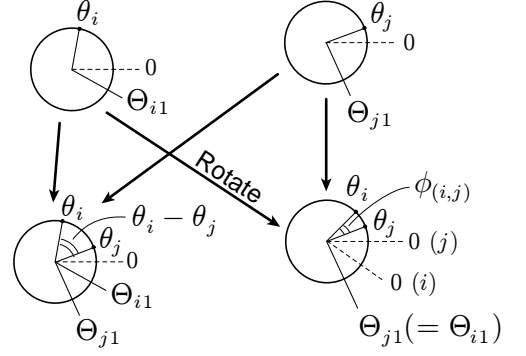


Fig. 5 Relations between two kinds of phase angle differences; $\theta_i - \theta_j$ and $\phi_{(i,j)}$.

tained,

$$\text{sign}(v_{l^*}^{i-1}, v_{l^*}^i) \cdot D_{(v_{l^*}^{i-1}, v_{l^*}^i)} = \begin{cases} -\frac{\Omega_{l^*} L_{(v_{l^*}^{i-1}, v_{l^*}^i)}}{v_{\max}}, & (q_{v_{l^*}^{i-1} \leftarrow v_{l^*}^i} \geq q_{v_{l^*}^i \leftarrow v_{l^*}^{i-1}}) \\ +\frac{\Omega_{l^*} L_{(v_{l^*}^i, v_{l^*}^{i-1})}}{v_{\max}}, & (q_{v_{l^*}^{i-1} \leftarrow v_{l^*}^i} < q_{v_{l^*}^i \leftarrow v_{l^*}^{i-1}}) \end{cases} \quad (28)$$

Equation (28) shows that the desired phase angle difference D in the oscillator model is proportional to the frequency of oscillation Ω . Thus, when a fixed desired offset (see Sec. 2.4) is given, we can still change the corresponding desired phase angle difference in the oscillator model by changing the frequency of oscillation of the signals.

Substituting (28) for (26), we obtain the condition of Ω_{l^*} for the sum of the desired phase angle differences D satisfying the closed-loop constraint, as,

$$\frac{\Omega_{l^*}}{v_{\max}} \Lambda_{l^*} + \sum_{i=1}^{|V(l^*)|} \Delta(v_{l^*}^{i-1}, v_{l^*}^i, (v_{l^*}^{i-1}, v_{l^*}^i)) = 2n\pi, \quad n \in \mathbb{Z}, \quad (29)$$

where Λ_{l^*} is defined as,

$$\Lambda_{l^*} = \sum_{i=1}^{|V(l^*)|} \chi(q_{v_{l^*}^{i-1} \leftarrow v_{l^*}^i}, q_{v_{l^*}^i \leftarrow v_{l^*}^{i-1}}) \cdot L_{(v_{l^*}^{i-1}, v_{l^*}^i)}. \quad (30)$$

In (30), χ is a function that gives a sign,

$$\chi(q_{v_{l^*}^{i-1} \leftarrow v_{l^*}^i}, q_{v_{l^*}^i \leftarrow v_{l^*}^{i-1}}) = \begin{cases} -1, & (q_{v_{l^*}^{i-1} \leftarrow v_{l^*}^i} \geq q_{v_{l^*}^i \leftarrow v_{l^*}^{i-1}}) \\ +1, & (q_{v_{l^*}^{i-1} \leftarrow v_{l^*}^i} < q_{v_{l^*}^i \leftarrow v_{l^*}^{i-1}}) \end{cases} \quad (31)$$

As shown in Fig. 6, χ is positive when the orientation of the main traffic flow (i.e. the larger one of the two counter-directional traffic flows) on the link $(v_{l^*}^{i-1}, v_{l^*}^i)$ is the same as the positive orientation of the loop l^* . When they are opposite to each other, χ is negative.

Λ_{l^*} is the sum of the product of the length of links and the sign χ along the loop l^* . $|\Lambda_{l^*}|$ attains the largest value when all the link have the main traffic flows with the same (positive or negative) orientation, forming a circulating traffic flow over the loop. When the links does not share one and the same orientation, $|\Lambda_{l^*}|$ attains a smaller value. When $\Lambda_{l^*} = 0$ and $\Delta = 0$ hold at the same time, (26) is satisfied for arbitrary Ω_{l^*} . On the other hand, (26) is not satisfied for any Ω_{l^*} when $\Lambda_{l^*} = 0$ and $\Delta \neq 0$ hold.

Equation (29) is rewritten as,

$$\Omega_{l^*} = \begin{cases} \frac{v_{\max}}{\Lambda_{l^*}} \left[2m\pi - \sum_{i=1}^{|V(l^*)|} \Delta \left(v_{l^*}^{i-1}, v_{l^*}^i, (v_{l^*}^{i-1}, v_{l^*}^i) \right) \right], & (\Lambda_{l^*} > 0) \\ \frac{v_{\max}}{-\Lambda_{l^*}} \left[2m\pi + \sum_{i=1}^{|V(l^*)|} \Delta \left(v_{l^*}^{i-1}, v_{l^*}^i, (v_{l^*}^{i-1}, v_{l^*}^i) \right) \right], & (\Lambda_{l^*} < 0) \end{cases} \quad (32)$$

where $m = 0, 1, 2, \dots$. When (32) holds, the closed-loop constraint in (26) is satisfied.

Equation (32) has multiple solutions of Ω_{l^*} . The interval between adjacent solutions is $\frac{2v_{\max}}{|\Lambda_{l^*}|}\pi$. When the total length of the loop is large and the main flows form a circulating flow along the loop, (32) has many solutions of Ω_{l^*} and the interval between the solutions is narrow.

It is noted that a solution with $\Omega_{l^*} < 0$ makes no sense in (32). When $\Lambda_{l^*} = 0$ and $\Delta = 0$ hold together, the closed-loop constraint in (26) is satisfied for arbitrary Ω_{l^*} , which is mentioned previously.

As it is mentioned in Sec. 2.4, while the previous paper [3] gives the desired phase angle difference $D_{(i,j)}$ as (18), the present paper gives $D_{(i,j)}$ as (16). This is due to the inconvenient property of the function in (18).

In the cycle length control, first we consider the closed-loop constraints on the desired phase angle difference $D_{(i,j)}$. Then we choose the appropriate value of the oscillation frequency Ω_{l^*} so that the sum of $D_{(i,j)}$ is satisfied. Now let us consider $D_{(i,j)}$ as a function Ω_{l^*} . In order to solve the closed-loop constraint on the loop, the range of $D_{(i,j)}$ is required to be $[0, 2\pi)$. Here let us inspect (18). Since $D_{(i,j)}$ is defined as the weighted interior division of $D_{i \leftarrow j}$ and $D_{j \leftarrow i}$ with $q_{i \leftarrow j}$ and $q_{j \leftarrow i}$ as respective weight coefficients, when $q_{i \leftarrow j} \simeq q_{j \leftarrow i}$, the range of $D_{(i,j)}$ is limited to a small fan-shaped region around $D_{(i,j)} = 0$ or $D_{(i,j)} = \pi$ (whether 0 or π is determined by the ratio of $L_{(i,j)}$ and v_{\max}). This means that the value of $D_{(i,j)}$ cannot be changed arbitrarily and therefore the closed-loop

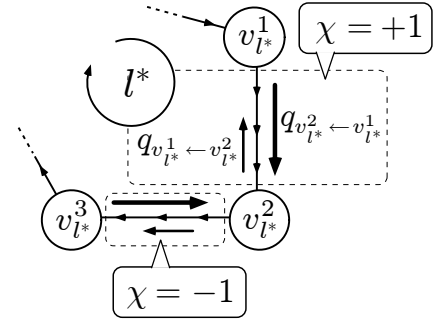


Fig. 6 Values of χ , determined by the orientation of the main traffic flow on the link with respect to the loop's positive orientation.

constraint is often not satisfied even how much we change the value of Ω_{l^*} . In the case of $D_{(i,j)}$ defined in (16), which we use here, $D_{(i,j)}$ is positive or negative proportional to Ω_{l^*} (the sign of the coefficient is determined by the main traffic flow on a road). Therefore the range of $D_{(i,j)}$ is always $D_{(i,j)} \in [0, 2\pi)$. We can solve the closed-loop constraint on offsets by changing the cycle length Ω_{l^*} .

3.3 Dynamics of loop managers

As mentioned in the previous subsection, (32) has a series of solutions with a constant interval. To determine the most appropriate among them, the following procedures are introduced. We first define a cosine-curved function for the local reaction potential as,

$$U_0(\Omega_{l^*}) = \begin{cases} -\frac{k_0 v_{\max}}{\Lambda_{l^* \max}} \cos \left[\frac{\Lambda_{l^*}}{v_{\max}} \Omega_{l^*} + \sum_{i=1}^{|V(l^*)|} \Delta \left(v_{l^*}^{i-1}, v_{l^*}^i, (v_{l^*}^{i-1}, v_{l^*}^i) \right) \right] & (\Lambda_{l^*} > 0) \\ -\frac{k_0 v_{\max}}{\Lambda_{l^* \max}} \cos \left[\frac{-\Lambda_{l^*}}{v_{\max}} \Omega_{l^*} - \sum_{i=1}^{|V(l^*)|} \Delta \left(v_{l^*}^{i-1}, v_{l^*}^i, (v_{l^*}^{i-1}, v_{l^*}^i) \right) \right] & (\Lambda_{l^*} < 0) \end{cases} \quad (33)$$

where k_0 is a convergence factor, and $\Lambda_{l^* \max}$ is a maximum value of Λ_{l^*} ,

$$\Lambda_{l^* \max} = \sum_{i=1}^{|V(l^*)|} L_{(v_{l^*}^{i-1}, v_{l^*}^i)}. \quad (34)$$

Governed by the gradient system of $U_0(\Omega_{l^*})$, Ω_{l^*} may attain one of the minima of $U_0(\Omega_{l^*})$, each of which corresponds to one of the solutions of (32). The allowed oscillation frequency of signals should be, however, neither too high nor too low to be realistic. In the present model, we introduce the allowed maximum and minimum, Ω_{\max}

and Ω_{\min} , respectively, to define an allowed band for Ω_{l^*} . A penalty function is introduced to let Ω_{l^*} remain within the allowed band $[\Omega_{\min}, \Omega_{\max}]$.

We must consider then the case that (32) does not have any solution of Ω_{l^*} within $[\Omega_{\min}, \Omega_{\max}]$. This will happen when the total length of the loop is short or the main traffic flows on the links do not obviously form a circulating flow along the loop. In this case, Ω_{l^*} will converge to a “pseudo” minimum, Ω_{\min} or Ω_{\max} , composed of the penalty function and $U_0(\Omega_{l^*})$. To avoid this, we introduce the following function as a potential,

$$U_1(\Omega_{l^*}) = \begin{cases} \frac{k_0 v_{\max}}{\Lambda_{l^* \max}} (\Omega_{l^*} - \Omega_{\max}), & (\Omega_{l^*} > \Omega_{\max}) \\ 0, & (\Omega_{\min} \leq \Omega_{l^*} \leq \Omega_{\max}) \\ \frac{k_0 v_{\max}}{\Lambda_{l^* \max}} (\Omega_{\min} - \Omega_{l^*}), & (\Omega_{l^*} < \Omega_{\min}) \end{cases} \quad (35)$$

In (35), there are no reaction term in the allowed band. Therefore Ω_{l^*} in the allowed band is governed by the diffusion term.

Next we consider the case that (32) has one or more solutions of Ω_{l^*} within $[\Omega_{\min}, \Omega_{\max}]$. We employ the following potential function as,

$$U_2(\Omega_{l^*}) = \begin{cases} \frac{k_0 v_{\max}}{\Lambda_{l^* \max}} (\Omega_{l^*} - \Omega_{l^* \text{top}}) + U_0(\Omega_{l^* \text{top}}), & (\Omega_{l^*} > \Omega_{l^* \text{top}}) \\ U_0(\Omega_{l^*}), & (\Omega_{l^* \text{bottom}} \leq \Omega_{l^*} \leq \Omega_{l^* \text{top}}) \\ \frac{k_0 v_{\max}}{\Lambda_{l^* \max}} (\Omega_{l^* \text{bottom}} - \Omega_{l^*}) + U_0(\Omega_{l^* \text{bottom}}), & (\Omega_{l^*} < \Omega_{l^* \text{bottom}}) \end{cases} \quad (36)$$

where $\Omega_{l^* \text{bottom}}$ and $\Omega_{l^* \text{top}}$ are

$$\Omega_{l^* \text{bottom}} = \max \left[\left(\Omega_{l^* \min} - \frac{v_{\max}}{|\Lambda_{l^*}|} \pi \right), \Omega_{\min} \right], \quad (37)$$

$$\Omega_{l^* \text{top}} = \min \left[\left(\Omega_{l^* \max} + \frac{v_{\max}}{|\Lambda_{l^*}|} \pi \right), \Omega_{\max} \right]. \quad (38)$$

In the above equations, $\Omega_{l^* \max}$ and $\Omega_{l^* \min}$ are the respective maximal and minimal solutions of (32) within $[\Omega_{\min}, \Omega_{\max}]$. The ordering of values of $\Omega_{l^* \max}$, $\Omega_{l^* \min}$, Ω_{\max} , and Ω_{\min} determines the values of $\Omega_{l^* \text{top}}$ and $\Omega_{l^* \text{bottom}}$. Two examples of $U_2(\Omega_{l^*})$ are shown in Fig. 7.

The local reaction potential for Ω_{l^*} is given as,

$$U(\Omega_{l^*}) = \begin{cases} U_1(\Omega_{l^*}), & \text{if the solution of (32)} \\ & \text{does not exist in } [\Omega_{\min}, \Omega_{\max}] \\ U_2(\Omega_{l^*}), & \text{if the solution of (32)} \\ & \text{exists in } [\Omega_{\min}, \Omega_{\max}] \end{cases} \quad (39)$$

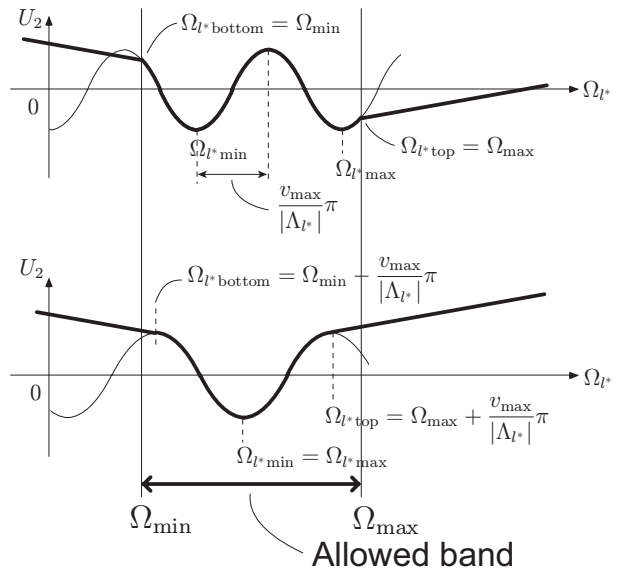


Fig. 7 Two examples of the potential U_2 . Top: The case in which $(\Omega_{l^* \min} - \frac{v_{\max}}{|\Lambda_{l^*}|} \pi) < \Omega_{\min}$ and $(\Omega_{l^* \max} + \frac{v_{\max}}{|\Lambda_{l^*}|} \pi) > \Omega_{\max}$ hold. Bottom: The case in which $(\Omega_{l^* \min} - \frac{v_{\max}}{|\Lambda_{l^*}|} \pi) > \Omega_{\min}$ and $(\Omega_{l^* \max} + \frac{v_{\max}}{|\Lambda_{l^*}|} \pi) < \Omega_{\max}$ hold.

We define the local diffusion potential for Ω_{l^*} to smooth off the oscillation frequencies of the neighboring loops as,

$$U_d(\Omega_{l^*}) = \sum_{k^* \sim l^*} k_1 (\Omega_{l^*} - \Omega_{k^*})^2. \quad (40)$$

where $k^* \sim l^*$ means that two loops k^* and l^* are neighboring, and k_1 is a convergence factor.

The reaction-diffusion equation of Ω_{l^*} composed of (39) and (40) is defined as,

$$\frac{d\Omega_{l^*}}{dt} = -\frac{\partial}{\partial \Omega_{l^*}} \sum_{l^* \in \bar{V}^*} \left\{ U(\Omega_{l^*}) + U_d(\Omega_{l^*}) \right\}. \quad (41)$$

The first term of the right-hand side of (41) is a reaction term representing the local demand of each loop, and the second term is a diffusion term representing the cooperation between the neighboring loops. Because the signals have almost uniform oscillation frequencies, which is mentioned in Sec. 3.1, the second term of the right-hand side of (41) should affect more strongly than the first term. Thus, the parameter k_1 in (40) should be set at a larger value than k_0 in (35) and (36).

3.4 Dynamics of signals

Equation (41) is the equation concerned with Ω_{l^*} (the oscillation frequency of the loops). We need the dynamics of the *frequency of the signals*, i.e. the dynamics of ω_i . We describe the method for controlling the oscillation frequency of the signals based on that of the loops.

At first, we define the set of loops that are “surround-

ing” the node $i \in G$ as,

$$\tilde{V}^*(i) = \left\{ l^* \in \tilde{V}^* \mid i \in V(l^*) \right\}. \quad (42)$$

The dynamics of the signals are given as,

$$\frac{d\omega_i}{dt} = -\frac{\partial}{\partial \omega_i} \sum_{i \in V} \left\{ \Upsilon(\omega_i) + \Upsilon_d(\omega_i) \right\} \quad (43)$$

$$\Upsilon(\omega_i) = \epsilon_0 \left\{ \omega_i - \frac{1}{|\tilde{V}^*(i)|} \sum_{l^* \in \tilde{V}^*(i)} \Omega_{l^*} \right\}^2, \quad (44)$$

$$\Upsilon_d(\omega_i) = \epsilon_1 \sum_{j \sim i} (\omega_i - \omega_j)^2, \quad (45)$$

where ϵ_0 and ϵ_1 are the convergence factors.

Equation (44) shows that each signal moves its oscillation frequency toward the average value for the frequencies of the surrounding loops. Equation (45) means that the oscillation frequencies of the neighboring signals are smoothed off. It is noted that the oscillation frequencies of the *loops* are already smoothed off in (40). Since the almost uniform value of the oscillation frequencies is necessary for the present control method, we used the smoothing operation twice.

4. Simulations

4.1 Simulation environment

The environment used in this simulation is shown in Fig. 8. There are 5 parallel roads in north and south direction and 4 parallel ones for east and west with 20 signals. While our previous paper [3] has assumed the squared environment i.e., all the signals have the same distance between their neighbors, the distances between the signals are different in Fig. 8. The automobiles come from the outside. As for the traffic model, we use a discrete model that is the same in the paper [3].

Although our previous paper [3] has assumed that the traffic volume of each of the four directions is uniform in all of the parallel roads (e.g., $Q_{E1} = Q_{E2} = Q_{E3} = Q_{E4}$ in Fig. 8), the present paper does not assume it (e.g., the arriving traffic volume from north in “Avenue 1” in Fig. 8 is different from the one in “Avenue 2”).

It is noted that Λ_{l^*} in (30) is equal to 0 if traffic volume of each direction is uniform in all of the parallel roads and the environment is square, which are both assumed in [3]. In such situations, the splits of the signals will be almost uniform over all the signals, therefore $\Delta \simeq 0$ holds in (24). This shows that the closed-loop constraints on the offsets will be satisfied for arbitrary frequencies of oscillations in the case in [3].

The values of control parameters are shown in Table 1.

4.2 Simulation results

For $0 < t \leq 3000$ (s), the frequencies of car arrival are

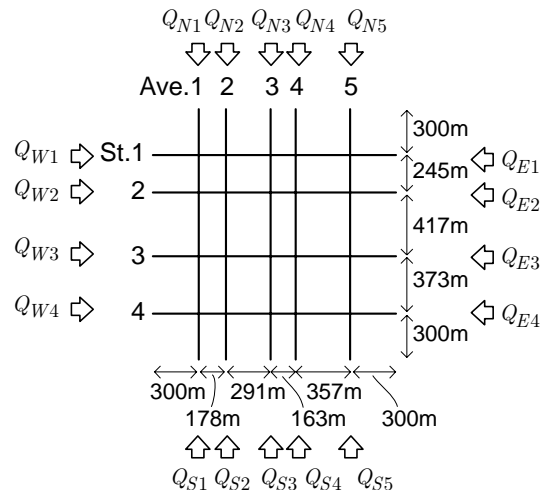


Fig. 8 Simulated environment.

Table 1 Simulation parameters.

α	0.002	ϵ_0	0.02
β	0.002	ϵ_1	0.1
γ	$\bar{\omega}_{(i,j)}/8.0$	Ω_{\max}	$2\pi/45$ (rad/s)
k_0	0.0015	Ω_{\min}	$2\pi/240$ (rad/s)
k_1	0.08		

set as shown in Fig. 9-(a), where “L”, “ML”, “M”, and “S” in the figure denote the frequency of arrival, 0.383 (1/s), 0.172 (1/s), 0.138 (1/s), and 0.057 (1/s), respectively. The traffic condition changes at $t = 3000$ (s), as shown in Fig. 9-(a). It is noted that the inflow traffic volumes from north and south in “Avenue 3” are turned over at $t = 3000$ (s). Figure 9 also illustrates the loop with circulating main traffic flows on the links by the symbols “ \circ ” and “ \ominus ”. The number of the loops with circulating traffic flow also changes at $t = 3000$ (s). The behavior of traffic signals and automobiles is calculated by the fourth order Runge-Kutta method.

Figure 10 shows the number of automobiles existing in the environment at time t . The proposed method is compared to the following control methods,

- control of splits with a fixed frequency of oscillation and offset ($\omega = 2\pi/120, \phi = 0$),
- control of splits and offsets proposed in our previous paper [3] with a fixed frequency of oscillation ($\omega = 2\pi/120$).
- control of splits and offsets in (16) with a fixed frequency of oscillation ($\omega = 2\pi/120$).

In Fig. 10, the present method, controlling all the three parameters, shows the lowest number of existing automobiles. This shows that the present method achieves the highest efficiency. The efficiency in the previous method is comparable to that in the split control only. The pre-

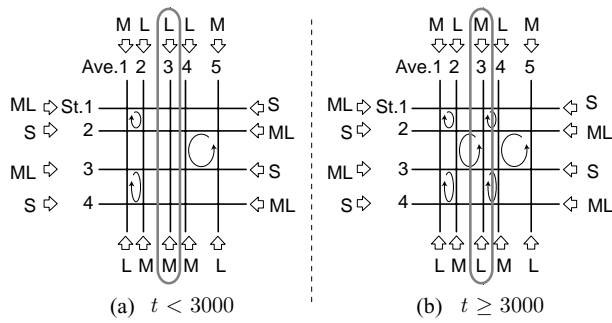


Fig. 9 Traffic conditions at the simulation. (a) Inflow traffic volumes at $t < 3000$ (s), where $L=0.383$ (1/s), $ML=0.172$ (1/s), $M=0.138$ (1/s), $S=0.057$ (1/s), all of which denote the frequencies of car arrival. (b) Inflow volumes at $t \geq 3000$ (s). The volume from the north and that from the south in “Avenue 3” are turned over. Symbols “○” or “◉” indicate the loops with rotating main traffic flows.

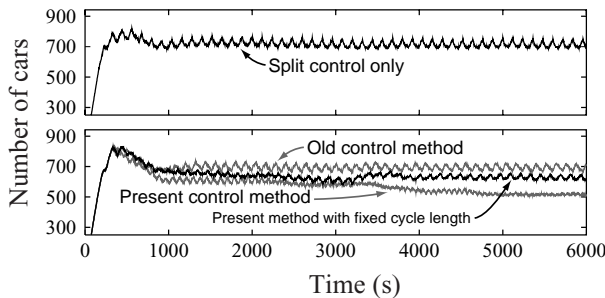


Fig. 10 Simulation results of four different control methods. Number of automobiles at time t in the environment.

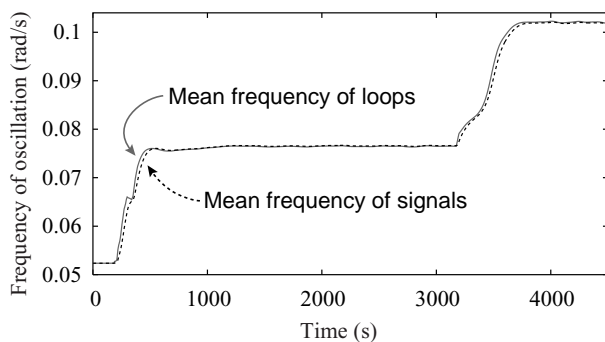


Fig. 11 Time evolutions of the mean value of Ω_{l^*} (frequency of loops) and ω_i (frequency of signals).

vious offset control method, therefore, is not effective in such environments experimented here. In the case with the present offset control method in (16) and fixed oscillation frequency, the efficiency is slightly higher than that in the split control only and that in the previous control method. New offset control method contributes to improve the traffic efficiency.

Figure 11 shows the average values of ω_i and Ω_{l^*} , frequency of oscillation of signals and that of loops, respec-

tively. We can see that ω_i follows after Ω_{l^*} quickly and that both ω_i and Ω_{l^*} shows stable behavior. The initial value is $2\pi/120 = 0.524$ (rad/s). At $t = 600$ (s), the system’s frequency is converged to 0.0764 (rad/s). In response to the change in traffic condition at $t = 3000$ (s), the system’s frequency is enhanced, converging to 0.102 (rad/s) at $t = 3700$ (s).

Further we find in Fig. 10, the number of automobiles in $t < 3000$ (s) is larger than that in $t \geq 3000$ (s), indicating that the efficiency of the former is lower than the latter. For the traffic condition in $t < 3000$ (s), the loops with circulating main traffic flows are three in number (see Fig. 9-(a)). This means that the majority of loops do not have solutions of the oscillation frequencies in (32). In this case, the efficiency enhancement is not so much as expected. In the condition for $t \geq 3000$ (s), there appear six loops with circulating main traffic flows. Here a significant improvement in the efficiency is actually seen, indicating the effectiveness of the appropriate control of the cycle length of the system.

5. Conclusion and future work

We have presented a decentralized method for controlling a large number of traffic signals. The model is extended to include the control of cycle length, along with the control of splits and offsets, which have been presented previously. The regulation of all the three parameters of each signal has successfully led to the enhancement of the efficiency of the system.

We explained the closed-loop constraint on a loop, where the convergence of the offsets into the desired offsets depends on the the cycle length of the signals. For this problem, we proposed to control the cycle lengths so that the desired offset will satisfy the closed-loop constraint. The loop managers, corresponding the unbounded faces of the graph one to one, have their own oscillation frequencies. The loop managers are governed by the reaction-diffusion equation on a dual graph. This method can control the cycle lengths of the signals according to the traffic condition, keeping the uniformity as a whole.

The next task is the further extension of the model, allowing for the traffic flows turning right or left, various types of intersections, the roads with multiple lanes, and so on. Since our model has no limitation on the degree of each node, the present control method has the potential for handling nodes with various degrees, along with the 4-degree nodes (i.e. crossroad intersections). Nishikawa and Kita have proposed the extension of the offset control in [5], which is useful for us. As for the split and the

cycle length, the extension of the control method should be developed hereafter. The endeavor along this direction will enable us to apply the present approach to the actual road networks.

We used 2-phase cycle as the cycle system of the signals. In a large intersection with traffic flows turning right or left, the signal of the intersection will need three or more phases in a cycle. In this case, we need vector for representing the split of a signal, instead of scalar. The dynamics of Hamilton system on a graph, which can handle vector, should be developed.

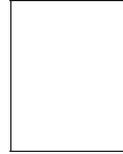
Acknowledgements

We thank Prof. Hajime Kita, National Institution for Academic Degrees, and Prof. Ikuko Nishikawa, Ritsumeikan University, for their valuable suggestions.

References

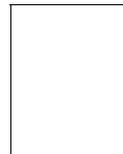
- 1) Tsutomu Usami and Hajime Sakakibara: Traffic Control System in Road Network, *Journal of the SICE*, Vol. 41, No. 3, pp.205–210, 2002 (in Japanese).
- 2) S. Kawakami and H. Matsui: *Traffic Engineering*, Morikita Shuppan Co., 1987 (in Japanese).
- 3) M. Sugi, H. Yuasa, T. Arai: Autonomous Distributed Control of Traffic Signal Network, *Transactions of the SICE*, Vol.39, No.2, pp.51–58 2003 (in Japanese).
- 4) K. Sekiyama, J. Nakanishi, I. Takagawa, T. Higashi, T. Fukuda: Self-Organization of Offset Pattern in Urban Traffic Signal Network, *Proc. 13th SICE Symposium on Decentralized Autonomous Systems*, 45/50, 2001 (in Japanese).
- 5) Ikuko Nishikawa, Shigeto Nakazawa, Hajime Kita: Area-wide Control of Traffic Signals by a Phase Model, *Transaction of the SICE*, Vol.39, No.2, 199/208, 2003 (in Japanese).
- 6) Tatsuro Mitsui: Traffic Signal Control, *JIDOSHA GIJUTSU (Journal of Society of Automotive Engineers of Japan)*, Vol.54, No.7, pp.67–72, 2000 (in Japanese).
- 7) Sadayoshi Mikami, Yukinori Kakazu: Traffic Signals Control by Multi-Agent Reinforcement Learning, *Proceedings of the JSME Spring Annual Meeting*, Vol.1, pp.126–128, 1994 (in Japanese).
- 8) Tadanobu MISAWA, Haruhiko KIMURA, Sadaki HIROSE, and Nobuyasu OSATO: Multiagent-based Traffic Signal Control with Reinforcement Learning, *Transactions on IEICE*, Vol. J83-D-I, No.5, pp.478–486, 2000 (in Japanese).
- 9) H. Yuasa and M. Ito: Autonomous Decentralized Systems and Reaction-Diffusion Equation on a Graph, *Transactions of the SICE*, Vol.35, No.11, 1447/1453, 1999 (in Japanese).
- 10) Jee-Hyong Lee and Hyoung Lee-Kwang: Distributed and Cooperative Fuzzy Controllers for Traffic Intersections Group, *IEEE Transactions on Systems, Man, and Cybernetics C*, Vol.29, No.2, pp.263–271 (1999).

Masao SUGI (Member)



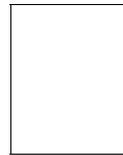
Masao Sugi received the B.E. degree in 1998 and the M.E. and Ph.D. degrees in 2000 and 2003, respectively, from the University of Tokyo. He is currently a Research Associate with the University of Tokyo. Dr. Sugi received the 2004 SICE paper award. He is a member of the Japan Society for Precision Engineering, the Robotics Society of Japan, and the IEEE Robotics and Automation Society.

Hideo YUASA (Member)



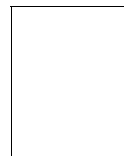
Hideo Yuasa received the B.S, M.S and Ph.D degrees from Nagoya University, in 1984, 1986 and 1992, respectively. He was the Assistant Professor in Department of Electronic-Mechanical Engineering, Nagoya University from 1992 to 1999. In 1999, he became an Associate Professor in Department of Precision Engineering, the University of Tokyo. He has been a Visiting Researcher in Bio-Mimetic Control Research Center, RIKEN, since 1993. His speciality was mathematical models and applications of distributed autonomous systems. He died suddenly in September 2002.

Jun OTA (Member)



Jun Ota received the M.Eng and Ph.D. degrees from Department of Precision Engineering, the University of Tokyo, in 1989 and 1994, respectively. He was with the Nippon Steel Co. Ltd. from 1989 to 1991. In 1991, he was a Research Associate of the University of Tokyo. In 1996, he became an Associate Professor in Department of Precision Engineering, the University of Tokyo. From 1996 to 1997, he was a Visiting Scholar in Stanford University. His research interests are multiple mobile robot systems, environmental design for robot systems, human-robot interface, and cooperative control of multiple robots.

Tamio ARAI (Member)



Tamio Arai received the Ph.D. degree in engineering from the University of Tokyo, Tokyo, Japan, in 1970. In 1987, he became a Professor in Department of Precision Engineering, the University of Tokyo. He worked in Department of Artificial Intelligence, the University of Edinburgh as a Visiting Researcher from 1979 to 1981. Since 2000, he has been a Director of Research into Artifacts, Center for Engineering, the University of Tokyo. His specialties are assembly and robotics, especially multiple mobile robots, including legged robot league of Robocup. Dr. Arai is an active member of CIRP, the Robotics Society of Japan, and the Japan Society for Automation Advancement.